



## RESEARCH LETTER

10.1002/2016GL071042

## Key Points:

- Individual black carbon particles extracted from Antarctic ice
- Single spherule black carbon aerosol particles found in modern rain and in ice cores dating both before and after industrialization
- Black carbon particles found with iron inclusions, suggesting a transport pathway for iron deposition in the Southern Ocean

## Supporting Information:

- Supporting Information S1

## Correspondence to:

R. Edwards,  
r.edwards@curtin.edu.au

## Citation:

Ellis, A., et al. (2016), Individual particle morphology, coatings, and impurities of black carbon aerosols in Antarctic ice and tropical rainfall, *Geophys. Res. Lett.*, 43, 11,875–11,883, doi:10.1002/2016GL071042.

Received 2 SEP 2016

Accepted 1 NOV 2016

Accepted article online 4 NOV 2016

Published online 19 NOV 2016

## Individual particle morphology, coatings, and impurities of black carbon aerosols in Antarctic ice and tropical rainfall

Aja Ellis<sup>1,2</sup>, Ross Edwards<sup>1</sup>, Martin Saunders<sup>3</sup>, Rajan K. Chakrabarty<sup>4</sup>, R. Subramanian<sup>2</sup>, Nicholas E. Timms<sup>5</sup>, Arie van Riessen<sup>1</sup>, Andrew M. Smith<sup>6</sup>, Dionisia Lambrinidis<sup>7</sup>, Laurie J. Nunes<sup>1</sup>, Paul Vallelonga<sup>8</sup>, Ian D. Goodwin<sup>9</sup>, Andrew D. Moy<sup>10,11</sup>, Mark A. J. Curran<sup>10,11</sup>, and Tas D. van Ommen<sup>10,11</sup>

<sup>1</sup>Physics and Astronomy, Curtin University, Perth, Western Australia, Australia, <sup>2</sup>Department of Mechanical Engineering, Carnegie Mellon University, Pittsburgh, Pennsylvania, USA, <sup>3</sup>Centre for Microscopy, Characterisation, and Analysis, University of Western Australia, Perth, Western Australia, Australia, <sup>4</sup>Department of Energy, Environmental & Chemical Engineering, Washington University in St. Louis, St. Louis, Missouri, USA, <sup>5</sup>Department of Applied Geology, Curtin University, Perth, Western Australia, Australia, <sup>6</sup>Australian Nuclear Science and Technology Organisation, Sydney, New South Wales, Australia, <sup>7</sup>Research Institute for the Environment and Livelihoods, Charles Darwin University, Darwin, Northern Territory, Australia, <sup>8</sup>Centre for Ice and Climate, Niels Bohr Institute, University of Copenhagen, Copenhagen, Denmark, <sup>9</sup>Marine Climate Risk Group, Department of Environmental Sciences, Macquarie University, Sydney, New South Wales, Australia, <sup>10</sup>Australian Antarctic Division, Kingston, Tasmania, Australia, <sup>11</sup>Antarctic Climate and Ecosystems Cooperative Research Centre, University of Tasmania, Hobart, Tasmania, Australia

**Abstract** Black carbon (BC) aerosols are a large source of climate warming, impact atmospheric chemistry, and are implicated in large-scale changes in atmospheric circulation. Inventories of BC emissions suggest significant changes in the global BC aerosol distribution due to human activity. However, little is known regarding BC's atmospheric distribution or aged particle characteristics before the twentieth century. Here we investigate the prevalence and structural properties of BC particles in Antarctic ice cores from 1759, 1838, and 1930 Common Era (C.E.) using transmission electron microscopy and energy-dispersive X-ray spectroscopy. The study revealed an unexpected diversity in particle morphology, insoluble coatings, and association with metals. In addition to conventionally occurring BC aggregates, we observed single BC monomers, complex aggregates with internally, and externally mixed metal and mineral impurities, tar balls, and organonitrogen coatings. The results of the study show BC particles in the remote Antarctic atmosphere exhibit complexity that is unaccounted for in atmospheric models of BC.

### 1. Introduction

Black carbon (BC) aerosols are primary particles emitted by fossil fuel combustion and biomass burning. They have a multitude of effects on the global atmosphere and Earth's surface, which result in the second largest contribution to climate change after carbon dioxide (CO<sub>2</sub>) [Bond et al., 2013]. Unlike CO<sub>2</sub> and methane gas (CH<sub>4</sub>), BC's atmospheric residence time is relatively short (weeks as opposed to decades) and its atmospheric concentration is highly variable [Kaufman et al., 2002]. BC emissions may have already contributed to large-scale changes in atmospheric circulation, with models suggesting that the Northern Hemisphere tropics expand linearly with increasing radiative forcing from BC emissions [Kovilakam and Mahajan, 2015]. The physical, chemical, and optical properties of BC are dynamic and evolve during atmospheric transport [Browne et al., 2015; Shen et al., 2014; Wang et al., 2014]. Estimates of BC climate sensitivity are complicated by hemispheric differences in both emission sources (fossil fuels or biomass burning) and coemitted chemical species, which coat and react with BC in the atmosphere. Indeed, BC from East Asian fossil fuel may be removed from the atmosphere faster than expected due to coemitted sulfate [Shen et al., 2014].

Morphologically, BC particles are semifractal aggregates composed of small, ~30 nm semigraphitic carbon nanospheres [Andreae and Gelencsér, 2006]. Graphitic carbon consists of randomly oriented graphite crystallites with a mean intercrystallite distance of 2.5 nm, embedded in a matrix of amorphous carbon [Franklin, 1950, 1951]. After emission, BC rapidly ages in the atmosphere. The fractal dimensions of BC aggregates increase, and their surfaces become coated and partially oxidized, affecting both their optical

properties and their interaction with water [McFiggans *et al.*, 2006; Oshima *et al.*, 2009]. The evolution of the BC surface from hydrophobic to hydrophilic has a major influence on its aerodynamic size, its removal from the atmosphere by wet deposition, and its subsequent transport and residence time in the atmosphere [Shen *et al.*, 2014]. Other insoluble particles may become externally and internally mixed with BC, thereby changing its optical properties [Scarnato *et al.*, 2015]. While there have been many characterization studies of freshly emitted BC aggregates [Chakrabarty *et al.*, 2006a; Chakrabarty *et al.*, 2006b; Pósfai *et al.*, 2003; Zhu *et al.*, 2013], few studies have investigated the morphology and characteristics of aged BC aggregates in the remote Southern Hemisphere (SH) [Pósfai *et al.*, 1999]. Consequently, the full range of properties of BC and their climate forcing effects remain uncertain. Furthermore, little is known with regard to historic records of atmospheric BC before the last few decades. Polar ice cores preserve an extensive history of atmospherically transported and aged BC particles and provide an opportunity to study changes in the physical and chemical properties of long-distance transported BC during and before the industrial revolution. Building upon the development of a method to concentrate BC particles in water [Ellis *et al.*, 2015], we investigated individual particles in an Antarctic ice core using electron microscopy.

Previous studies of BC in Antarctica have included bulk aerosol measurements, mass concentrations, and optical properties of Antarctic snow and ice [Bisiaux *et al.*, 2012; Warren and Clarke, 1990; Weller *et al.*, 2013; Wolff and Cachier, 1998]. These studies identified large seasonal variations in coastal East and West Antarctic BC aerosol concentrations with a primary peak in October that is associated with dry-season biomass burning on nearby continents. A smaller secondary peak in BC concentration is observed during austral summer fire season [Weller *et al.*, 2013] with minimum concentrations in March–April. High-temporal resolution ice core studies found similar seasonality in West and East Antarctic ice concentrations during the past 200 years [Bisiaux *et al.*, 2012]. The seasonality and atmospheric circulation associated with BC in the Antarctic atmosphere [Bisiaux *et al.*, 2012; Stohl and Sodemann, 2010] suggest that long-range transported SH biomass burning emissions are the primary source of BC to Antarctica.

Although ultratrace BC concentrations ( $0.08 \mu\text{g kg}^{-1}$ ) have been determined in Antarctic ice and snow, little is known with regard to individual particle morphology, coatings, and impurities. These characteristics impact the particles' optical and radiative properties, residence time in the atmosphere, and climatic impacts. Here we present results from the detailed analysis of individual particles found in an East Antarctic ice core and modern tropical rain samples from northern Australia. Three samples were prepared from ice core samples from the Law Dome ice cap, East Antarctica, dated from 1759, 1838, and 1930 Common Era (C.E.), predating and postdating global industrialization and western colonization of Australia. Tropical rain samples were collected in northern Australia to provide a complementary modern comparison to Antarctic ice, as wet-deposited BC close to potential source emissions. All samples were analyzed using high-resolution transmission electron microscope imaging (HR-TEM) and scanning transmission electron microscope energy-dispersive X-ray spectroscopy (STEM-EDS, hereafter EDS).

## 2. Materials and Methods

### 2.1. Ice Core Samples

Antarctic ice core samples consisted of ice sections subsampled from the Dome Summit South site (DSS0506,  $66^{\circ}46'S$ ,  $112^{\circ}48'E$ , 1370 m elevation) drilled on Law Dome, East Antarctica, during the 2005–2006 austral summer. The site has been described and studied in detail [Curran *et al.*, 1998; Edwards *et al.*, 2006; Etheridge *et al.*, 1996; van Ommen and Morgan, 1996]. The depth/age scale of the ice core was constructed by matching dissolved ion chemistry and water stable isotope records ( $\delta^{18}\text{O}$ ) to the main DSS ice core record, which was dated using annual layer counting and validated by well-characterized volcanic horizons [Plummer *et al.*, 2012].

### 2.2. Rain Samples

Tropical rain samples were collected in Darwin, Northern Territory, Australia, to compare modern BC in wet deposition, close to BC sources. Two rain samples of  $\sim 1$  L each were collected in April 2014, a period of significant monsoonal rainfall in the Northern Territory. Boundary layer atmospheric circulation to the sampling site during April 2014 was predominately east-west, passing over northern Queensland and the Gulf of Carpentaria before arriving in the Northern Territory.

Samples were collected in low-density polyethylene bottles, rinsed with ultrapure (UP) water ( $\rho > 18.2 \text{ M}\Omega \text{ cm}$ ). A full account of sample collection and handling is described in *Ellis et al.* [2015].

### 2.3. Ice Core Decontamination and Liquid Preconcentration

Mass concentrations of BC in Antarctic snow and ice are typically found in the parts per trillion level and require preconcentration before analysis by transmission electron microscopy (TEM). While Antarctic snow BC concentrations are low, the concentrations of other species, such as sea salts, may be present at the high parts per billion level, depending on the location. The presence of relatively high concentrations of dissolved salts species complicates sample preconcentration and obscures BC particles loaded on TEM grids. To concentrate BC particles from ice core samples and rain without concentrating dissolved salts, we used the tangential flow filtration (TFF) preconcentration method [*Ellis et al.*, 2015]. Meltwater from  $1 \text{ m} \times 5 \text{ cm} \times 5 \text{ cm}$  ice core sections, representing approximately 2 years of deposition to the site, was concentrated by approximately a factor of 1000 using hollow fiber filters (10 nm pore size, Spectrum Labs, USA). The TFF concentrate from each sample was transferred to a TEM grid (SPI 300-mesh gold grids with a continuous  $\text{SiO}/\text{SiO}_2$  support film) and evaporated down within an ISO 10 clean hood. Tropical rainwater samples were processed identically to the ice core meltwater.

### 2.4. TEM Characterization

Characterization (imaging of external morphology and internal structure, size, and composition) of the insoluble particles and their coatings was completed on an FEI Titan G2 80-200 TEM/STEM with ChemiSTEM Technology at The University of Western Australia, operating at 80 kV to minimize the risk of structural damage to the carbon spheres. High-angle annular dark-field scanning transmission electron microscopy (HAADF-STEM) imaging and element mapping were also carried out at 80 kV on the same instrument. The element maps were obtained by energy-dispersive X-ray spectroscopy using the Super-X detector on the Titan with a subnanometer probe size, a probe current of  $\sim 0.25 \text{ nA}$ , a dwell time of 15 ms, and total acquisition time of 20 to 30 min. Statistical evaluation of the proportions and size distribution of the various BC morphologies was inhibited because the TEM grids were not surveyed systematically—irregular deposition of particles on the grids and the limited field of view ( $< 10 \mu\text{m}$ ) resulting from the high magnification of the instrument makes location and characterization of BC particles time intensive, and acquisition of significant BC morphotype population statistics difficult. Therefore, the images selected for this paper represent common BC morphologies and characteristics seen while imaging the TEM grid. Images of additional particle types can be found in the supporting information.

## 3. Results

In all samples, abundant single BC nanospheres (Figure 1) in addition to conventional multispherule aggregates were observed. The nanoparticles were identified by their  $\sim 30 \text{ nm}$  diameter, concentric “onion” carbon layering with short-range order, and the  $K\alpha$  carbon peak in the EDS spectra. Single BC nanospheres are not thought to exist individually in the atmosphere [*Andreae and Gelencsér*, 2006] and to our knowledge have not previously been observed in ice or snow. However, their presence in Antarctic ice suggests that they must be ubiquitous in the global atmosphere. Because of their small size and the confounding presence of larger BC aggregates and other dust particles, the single spheres are difficult to discern without the use of STEM-EDS mapping. They have too little mass to be quantified by real-time single BC particle analysis instruments used in other studies [*Slowik et al.*, 2007]. It would be difficult to distinguish the single nanospheres in the presence of concentrated salts or sulfates. The preconcentration method used in this study removes dissolved salts and other water-soluble species, retaining insoluble particles. Our method is also extremely gentle (mechanically) and unlikely to provide enough mechanical force to separate the aggregates [*Rothenbacher et al.*, 2008]. Further investigation has revealed many examples of doublet and triplet BC nanospheres of various primary particle sizes (Figures 1b–1d). Single BC nanospheres were found in all ice core samples (dated to 1759, 1838, and 1930 C.E.) via HR-TEM. The rain samples also contained all of the nanosphere varieties that were seen in the ice cores, indicating their possible global presence.

Although quantification is difficult for irregularly distributed nanoparticles on TEM grids, a preliminary estimate of the prevalence of single BC nanospheres can be obtained using a single particle soot

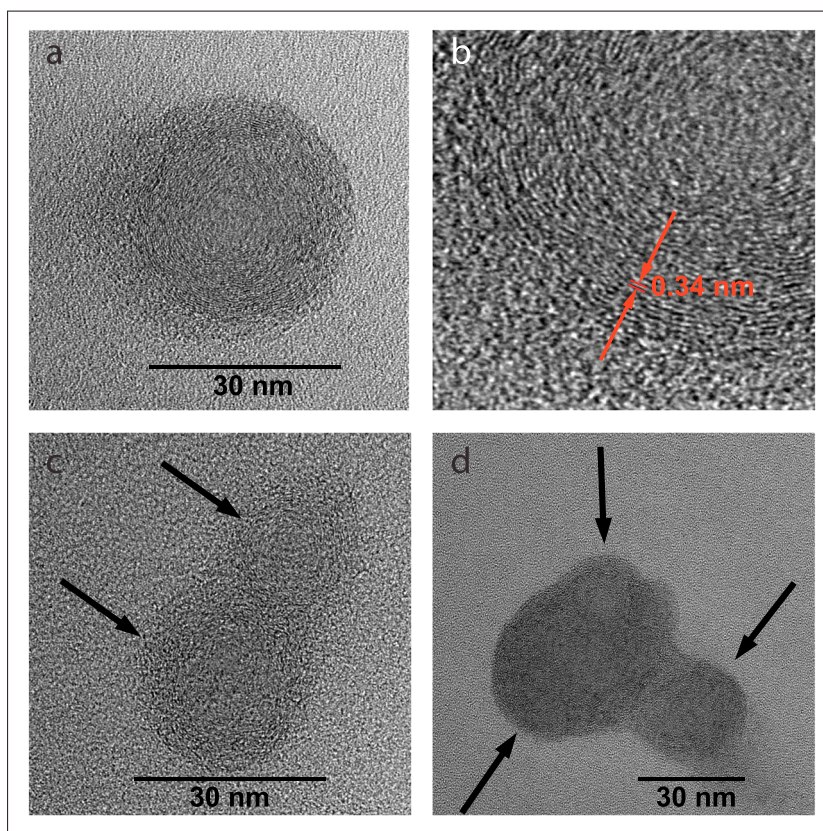


**Figure 1.** Black carbon nanospheres in Antarctic ice dated to 1838 C.E.: (a) single BC nanosphere showing concentric ring structure with short-range internal structure, (b) enlarged section of Figure 1a, showing the concentric layers with 0.34 nm spacing between layers, (c) BC particle with two spherules, arrows indicating spheres, and (d) BC particle with three spherules, arrows indicating spheres. Additional examples of single spheres from 1759 CE and 1930 CE are included in the supporting information.

photometer (SP2, Droplet Measurement Technologies). Indeed, BC size distribution data in twentieth century ice from the same location in East Antarctica indicate that a substantial fraction of BC particles exists below the below 0.7 fg (90 nm mass-equivalent diameter assuming a BC density of  $1.8 \text{ g/cm}^3$ ), the lower mass limit where the SP2 begins to detect less than 100% of BC aerosols, supporting the existence of these individual nanospheres in great numbers—primary nanospheres may outnumber the larger BC aggregates that have previously been reported.

This observation raises significant questions about the prevalence of single BC nanospheres, as well as the undescribed effects of single nanospheres on the environment. Modern scattering calculations for BC suggest that variations in size distribution, composition, or shape could have substantial effects on common spherical and Rayleigh-Debye-Gans simplifications [Smith and Grainger, 2014]. Though the individual nanospheres are likely to be too small to function as cloud condensation nuclei, aerosol chamber experiments have shown 30 nm metallic nanoparticles [Saunders et al., 2010] as well as conventional BC aggregates [DeMott et al., 1999] acting as ice nuclei in the atmosphere. This suggests the possibility that individual 30 nm BC nanospheres may contribute to the formation of ice particles in the atmosphere, thereby having an as yet unmeasured climate affect.

In addition to the single spherules, many other distinct BC characteristics were observed in the ice cores. We found a continuum of BC aggregate sizes ranging from doublet and triplet BC spherules (Figures 1c and 1d) up to many hundred nanometers (Figures 2 and 3). While the fractal dimension of the aggregates was not determined, they appeared to be relatively compact as would be expected of BC that has been substantially aged in the atmosphere and suspended in liquid water during the concentration procedure. All BC aggregates exhibited some form of thin insoluble coating ( $\sim 5 \text{ nm}$ ) that connected the individual spherules, similar



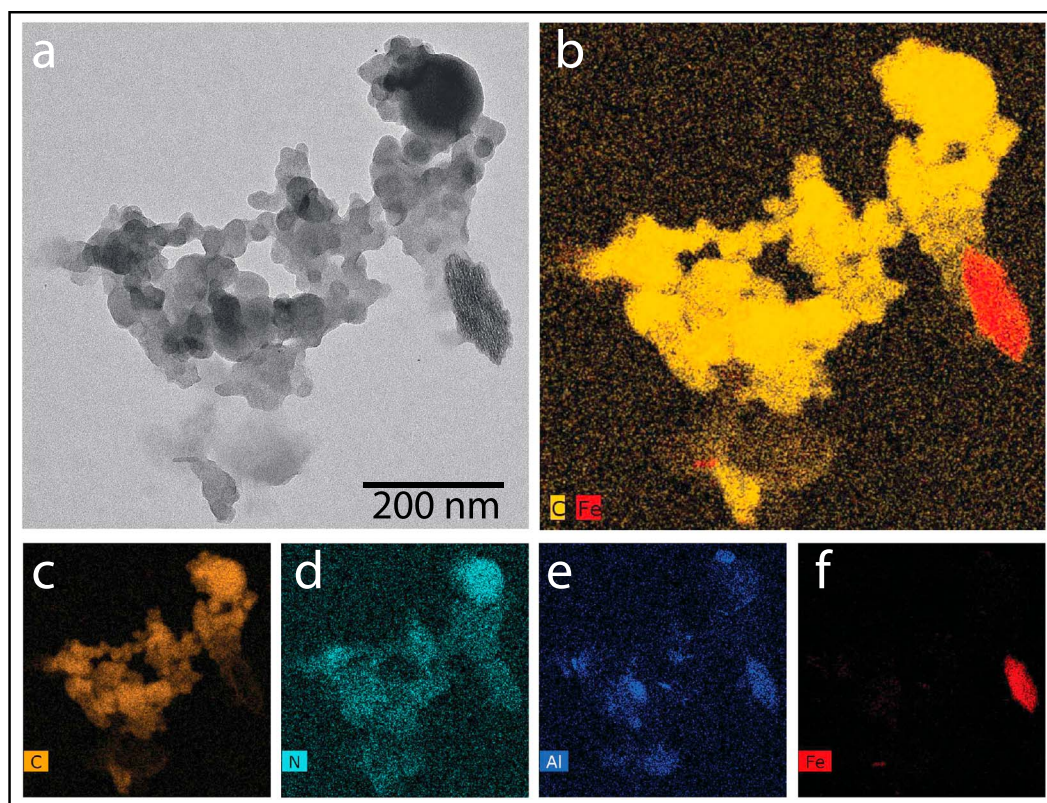


**Figure 2.** TEM images and STEM-EDS maps to show compositional complexity of a black carbon aggregate, from ice dated to 1838 C.E., with EDS maps taken from the same field of view as Figure 2a. (a) TEM image of BC aggregate, with tar ball incorporated into the aggregate, (b) STEM-EDS map overlay of carbon and iron, to highlight the iron particle connected with a carbon coating, (c) carbon map, (d) nitrogen map, (e) various aluminum-rich inclusions within the BC aggregate, and (f) iron map.

to the thin “film” of carbon found on remote BC aerosols by Pósfai *et al.* [1999]. EDS analysis revealed that the coatings appear to be composed predominately of amorphous carbon combined with varying amounts of nitrogen and oxygen-rich materials. These coatings appeared to be unaffected by high vacuum ( $10^{-5}$  Pa) or an 80 kV electron beam. While we have no definitive way of ascertaining when the coatings formed, it is likely that coatings are part of the atmospheric aging process and may have formed through aqueous cloud chemistry [Lee *et al.*, 2013]. The presence of oxygen in the coatings suggests that they are hydrophilic. The presence of a thin hydrophilic coating influences the BC particles’ interaction with atmospheric water, its atmospheric residence time, and optical properties.

Coated BC aggregates were routinely found in association with mineral dust particles composed of aluminum-rich silicates and iron. Magnesium, potassium, and zinc were also present in some attached minerals (Figure S6 in the supporting information). Many of the dust particles were found to be connected to the outside of BC aggregates by thin films of carbon, nitrogen, and oxygen (Figures 2b and 4), as well as being incorporated within the BC aggregate structure (Figure 3b). The external connections of the BC to the dust particles suggest that they are ice residual nuclei, as expected of wet-deposited BC in ice cores. Mineral dusts are common ice nuclei [DeMott *et al.*, 2003], and ice crystal scavenging of BC could explain the external connection [Baumgardner *et al.*, 2008].

Small iron particles (~10 nm in diameter) were often found adhered to the surface of BC aggregates (Figures 3 and 5). These attachments can be difficult to distinguish without the use of EDS or HAADF-STEM, in which heavier element inclusions stand out brightly.

BC has previously been imaged with larger dust particles in East Asian outflows [Clarke *et al.*, 2004] and African biomass burning plumes [Li *et al.*, 2003], and the results of our study show that external BC and dust



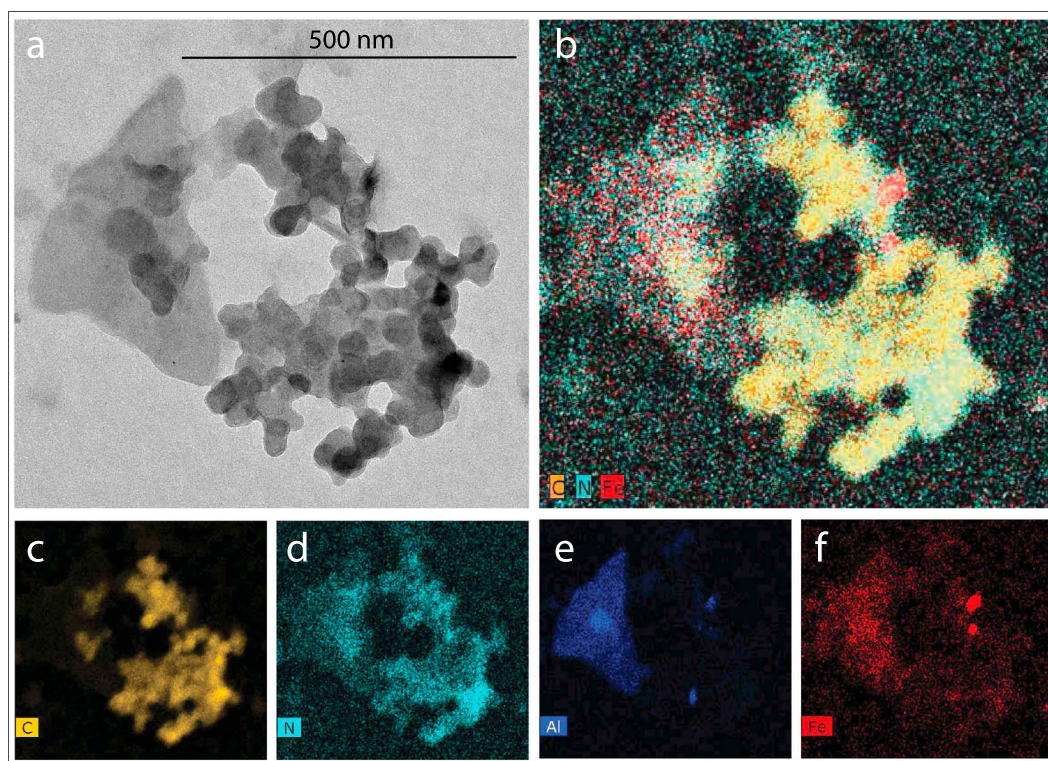


**Figure 3.** Dust particle and BC aggregate dated to 1838 C.E., with aluminum and iron dust particles incorporated within the BC aggregate, and EDS maps taken from the same field of view as Figure 3a. (a) TEM image, (b) carbon, nitrogen, and iron STEM-EDS maps overlaid to show the connection of the iron particles to the BC aggregate with a nitrogen-rich coating, (c–f) carbon, nitrogen, aluminum, and iron STEM-EDS maps, respectively.

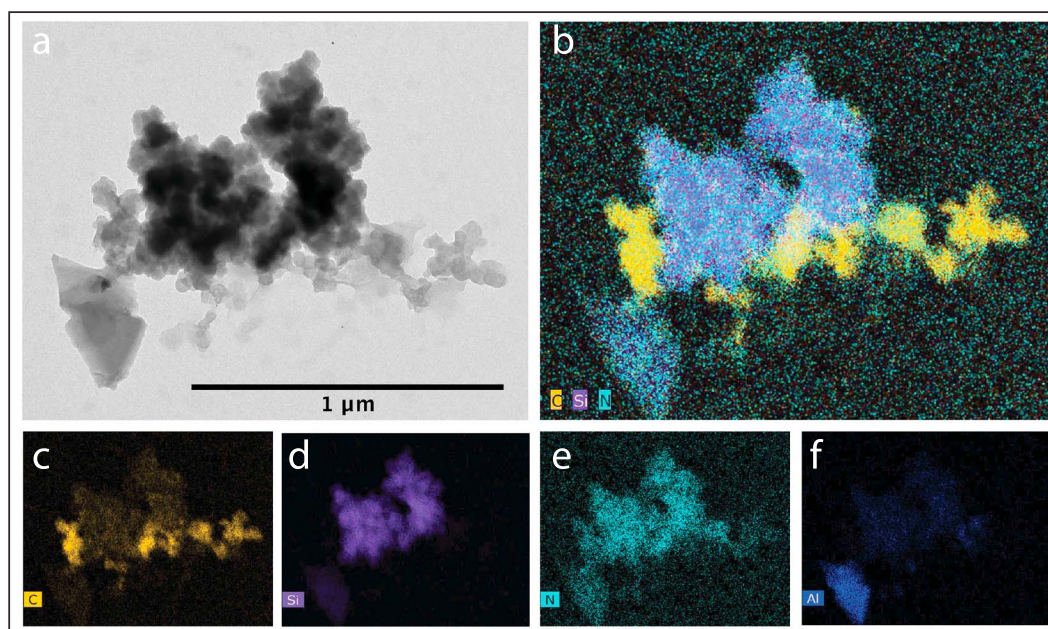


**Figure 4.** Large silica-rich dust particle from ice dated to 1838 C.E., with BC attached and mixed into the silica structure, with all components connected with thin (<5 nm), amorphous carbon and nitrogen-rich coating, with EDS maps taken from the same field of view as Figure 4a. (a) TEM image, (b) carbon, silicon, and nitrogen STEM-EDS maps overlaid to show connection of silicon and BC aggregates, with nitrogen-rich coating, (c–f) carbon, silicon, nitrogen, and aluminum STEM-EDS maps, respectively.

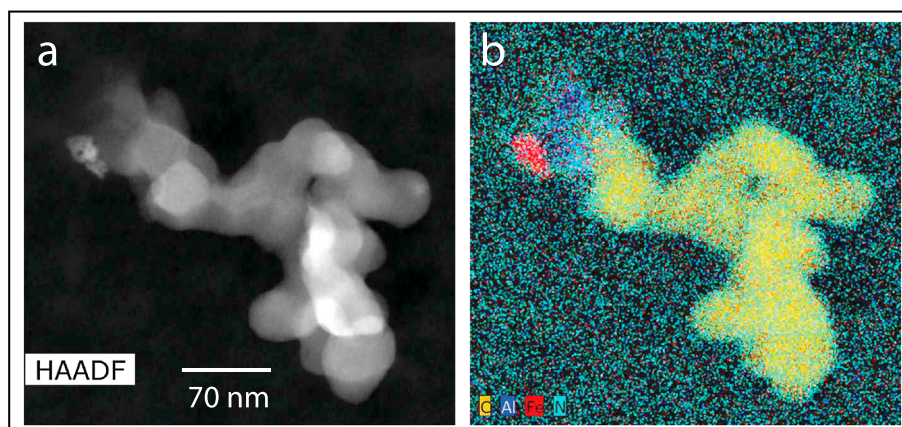


**Figure 5.** BC aggregate from ice dated to 1930 C.E. attached to aluminosilicate and iron particles with nitrogen-rich coating, with EDS map taken from the same field of view as Figure 5a. (a) High-angle annular dark-field (HAADF) image of the particle, (b) energy-dispersive X-ray spectroscopy (EDS) maps of C, Al, Fe, and N, indicating the aluminosilicate and iron particles are attached to the black carbon aggregate with a nitrogen-rich coating.

can be connected by insoluble coatings and can be transported long distances without disaggregating. These organic coatings and dust inclusions may have significant effects on BC's optical properties as well as functioning as cloud and ice nuclei in the atmosphere [Lohmann and Diehl, 2006].

The iron attached to the BC is of particular interest with respect to the biogeochemistry of iron in surface waters of the SH and potentially for the formation of water insoluble organic coatings through catalytic polymerization of organic species in biomass burning plumes [Slikboer et al., 2015].

Tar balls, amorphous, carbon-rich spheres emitted from smoldering fires, also accompanied the BC aggregates, both attached to the outside (Figure 6) and incorporated within the BC aggregates (Figure 2). Chakrabarty et al. [2006b] noted the existence of tar balls in laboratory combustion tests of biomass fuels, supporting their formation at the emission source. The presence of tar balls in Antarctic ice suggests that the particles were emitted by smoldering biomass burning [Adachi and Buseck, 2011; Chakrabarty et al., 2010]. To the best of our knowledge, this is the first determination of tar balls in Antarctica. They represent a previously unaccounted for component of light absorbing aerosols deposited to the Antarctic ice sheet. If tar balls are present in Antarctic ice, then they are likely present in air masses over the Southern Ocean

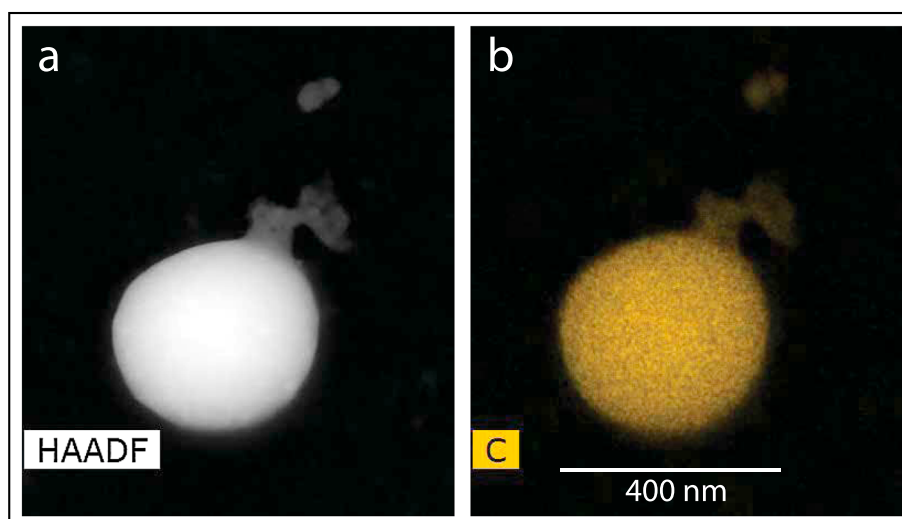


**Figure 6.** (a) High-angle annular dark-field (HAADF) image of a tar ball from ice dated to 1838 C.E. with BC aggregate attached, (b) EDS map of carbon from the same field of view as Figure 6a. Additional EDS maps are included in the supporting information.



and, presumably, the global troposphere. Further evidence of coatings, dust and metals, and single BC nanospheres in all samples are provided in the supporting information, as well as all additional STEM-EDS element maps for the particles described above.

#### 4. Conclusions

In this study we found evidence for the deposition of single black carbon (BC) nanospheres over East Antarctica and northern Australia. By extrapolation, we would expect to find these particles throughout the Southern Hemisphere, if not globally. The presence of single BC nanospheres in Antarctic ice dated to 1759 C.E., prior to industrialization, suggests that the source is likely grass or bush fires. We also found tar balls and BC with nitrogen and oxygen-rich insoluble coatings and associated with mineral particles and iron. The coatings appear to cover and connect the BC and many of the mineral particles. This suggests that the coatings and dust inclusions could form in a number of ways: rapidly close to the fire source, due to aqueous chemistry, and physical and chemical ice formation processes. These mixed particles also undergo long-range transport without disaggregating. The impact of the coatings and the external and internal mixing of the mineral particles may impact BC's optical properties and residence time in the atmosphere.

Knowledge of the long-range evolution of BC aerosol characteristics is critical for predicting the associated climate forcing. Mineral inclusions, metal impurities, and insoluble, nitrogen-rich coatings suggest a complex evolution in BC optical properties during transport. The diversity of particle properties observed in this study demonstrates the complexity of BC in the environment that is as yet unaccounted for in atmospheric chemistry and climate models.

The BC particles analyzed by the study did not display discernable differences between the different time periods, which may reflect the biomass burning-dominated emissions from the Southern Hemisphere. However, the small sample number and limited time span precludes conclusions regarding any systematic changes to BC morphology from the preindustrial period through the twentieth century. Northern Hemisphere shifts from natural biomass burning to anthropogenic industrial emissions during the industrial revolution could be recorded in BC characteristics, suggesting Arctic ice core investigations as an important future application of this study.

#### Acknowledgments

The data used will be available online at the Australian Antarctic Data Centre repository at <https://data.aad.gov.au/>. This work was supported by Australian Antarctic Sciences grant 4144, Curtin University grant RES-SE-DAP-AW-47679-1, and ARC LIEF grant LE130100029. The authors acknowledge the use of Curtin University's Microscopy and Microanalysis Facility, whose instrumentation has been partially funded by the University, State, and Commonwealth Governments. The authors acknowledge the facilities and the scientific and technical assistance of the Australian Microscopy and Microanalysis Research Facility at the Centre for Microscopy, Characterisation and Analysis, University of Western Australia, a facility funded by the University, State, and Commonwealth Governments.

#### References

- Adachi, K., and P. R. Buseck (2011), Atmospheric tar balls from biomass burning in Mexico, *J. Geophys. Res.*, *116*, D05204, doi:10.1029/2010JD015102.
- Andreae, M. O., and A. Gelencsér (2006), Black carbon or brown carbon? The nature of light-absorbing carbonaceous aerosols, *Atmos. Chem. Phys.*, *6*, 3131–3148, doi:10.5194/acp-6-3131-2006.
- Baumgardner, D., R. Subramanian, C. Twohy, J. Stith, and G. Kok (2008), Scavenging of black carbon by ice crystals over the northern Pacific, *Geophys. Res. Lett.*, *35*, L22815, doi:10.1029/2008GL035764.
- Bisiaux, M. M., R. Edwards, J. R. McConnell, M. A. J. Curran, T. D. Van Ommen, A. M. Smith, T. A. Neumann, D. R. Pasteris, J. E. Penner, and K. Taylor (2012), Changes in black carbon deposition to Antarctica from two high-resolution ice core records, 1850–2000 AD, *Atmos. Chem. Phys.*, *12*, 4107–4115, doi:10.5194/acp-12-4107-2012.
- Bond, T. C., S. J. Doherty, D. Fahey, P. Forster, T. Berntsen, B. DeAngelo, M. Flanner, S. Ghan, B. Kärcher, and D. Koch (2013), Bounding the role of black carbon in the climate system: A scientific assessment, *J. Geophys. Res.: Atmos.*, *118*, 5380–5552, doi:10.1002/jgrd.50171.
- Browne, E. C., J. P. Franklin, M. R. Canagaratna, P. Massoli, T. W. Kirchstetter, D. R. Worsnop, K. R. Wilson, and J. H. Kroll (2015), Changes to the chemical composition soot from heterogeneous oxidation reactions, *J. Phys. Chem. A*, *119*, 1154–1163, doi:10.1021/jp511507d.
- Chakrabarty, R., H. Moosmüller, L.-W. Chen, K. Lewis, W. Arnott, C. Mazzoleni, M. Dubey, C. Wold, W. Hao, and S. Kreidenweis (2010), Brown carbon in tar balls from smoldering biomass combustion, *Atmos. Chem. Phys.*, *10*, 6363–6370, doi:10.5194/acp-10-6363-2010.
- Chakrabarty, R. K., H. Moosmüller, W. P. Arnott, M. A. Garro, and J. Walker (2006a), Structural and fractal properties of particles emitted from spark ignition engines, *Environ. Sci. Technol.*, *40*, 6647–6654, doi:10.1021/Es060537y.
- Chakrabarty, R. K., H. Moosmüller, M. A. Garro, W. P. Arnott, J. Walker, R. A. Susott, R. E. Babbitt, C. E. Wold, E. N. Lincoln, and W. M. Hao (2006b), Emissions from the laboratory combustion of wildland fuels: Particle morphology and size, *J. Geophys. Res.*, *111*, D07204, doi:10.1029/2005JD006659.
- Clarke, A. D., et al. (2004), Size distributions and mixtures of dust and black carbon aerosol in Asian outflow: Physicochemistry and optical properties, *J. Geophys. Res.*, *109*, D15509, doi:10.1029/2003JD004378.
- Curran, M. A., T. D. Van Ommen, and V. Morgan (1998), Seasonal characteristics of the major ions in the high-accumulation Dome Summit South ice core, Law Dome, Antarctica, *Ann. Glaciol.*, *27*, 385–390, doi:10.3198/1998AoG27-1-385-390.
- DeMott, P. J., Y. Chen, S. M. Kreidenweis, D. C. Rogers, and D. E. Sherman (1999), Ice formation by black carbon particles, *Geophys. Res. Lett.*, *26*(16), 2429–2432, doi:10.1029/1999GL900580.
- DeMott, P. J., D. J. Cziczo, A. J. Prenni, D. M. Murphy, S. M. Kreidenweis, D. S. Thomson, R. Borys, and D. C. Rogers (2003), Measurements of the concentration and composition of nuclei for cirrus formation, *Proc. Natl. Acad. Sci. U.S.A.*, *100*(25), 14,655–14,660, doi:10.1073/pnas.2532677100.



- Edwards, R., P. Sedwick, V. Morgan, and C. Boutron (2006), Iron in ice cores from Law Dome: A record of atmospheric iron deposition for maritime East Antarctica during the Holocene and Last Glacial Maximum, *Geochem. Geophys.*, *7*(12), 3907–3910, doi:10.1029/2006GC001307.
- Ellis, A., et al. (2015), Characterizing black carbon in rain and ice cores using coupled tangential flow filtration and transmission electron microscopy, *Atmos. Meas. Tech.*, *8*(9), 3959–3969, doi:10.5194/amt-8-3959-2015.
- Etheridge, D., L. Steele, R. Langenfelds, R. Francey, J. M. Barnola, and V. Morgan (1996), Natural and anthropogenic changes in atmospheric CO<sub>2</sub> over the last 1000 years from air in Antarctic ice and firn, *J. Geophys. Res.*, *101*(D2), 4115–4128, doi:10.1029/95JD03410.
- Franklin, R. E. (1950), On the structure of carbon, *J. Chim. Phys. Phys.-Chim. Biol.*, *47*, 573–575.
- Franklin, R. E. (1951), The structure of graphitic carbons, *Acta Crystallogr.*, *4*(3), 253–261.
- Kaufman, Y. J., D. Tanre, and O. Boucher (2002), A satellite view of aerosols in the climate system, *Nature*, *419*(6903), 215–223, doi:10.1038/nature01091.
- Kovilakam, M., and S. Mahajan (2015), Black carbon aerosol-induced Northern Hemisphere tropical expansion, *Geophys. Res. Lett.*, *42*, 4964–4972, doi:10.1002/2015GL064559.
- Lee, A. K. Y., R. Zhao, R. Li, J. Liggio, S.-M. Li, and J. P. D. Abbatt (2013), Formation of light absorbing organo-nitrogen species from evaporation of droplets containing glyoxal and ammonium sulfate, *Environ. Sci. Technol.*, *47*(22), 12,819–12,826, doi:10.1021/es402687w.
- Li, J., M. Pósfai, P. V. Hobbs, and P. R. Buseck (2003), Individual aerosol particles from biomass burning in southern Africa: 2. Compositions and aging of inorganic particles, *J. Geophys. Res.*, *108*(D13), 8484, doi:10.1029/2002JD002310.
- Lohmann, U., and K. Diehl (2006), Sensitivity studies of the importance of dust ice nuclei for the indirect aerosol effect on stratiform mixed-phase clouds, *J. Atmos. Sci.*, *63*(3), 968–982, doi:10.1175/JAS3662.1.
- McFiggans, G., et al. (2006), The effect of physical and chemical aerosol properties on warm cloud droplet activation, *Atmos. Chem. Phys.*, *6*(9), 2593–2649, doi:10.5194/acp-6-2593-2006.
- Oshima, N., M. Koike, Y. Zhang, and Y. Kondo (2009), Aging of black carbon in outflow from anthropogenic sources using a mixing state resolved model: 2. Aerosol optical properties and cloud condensation nuclei activities, *J. Geophys. Res.*, *114*, 2156–2202, doi:10.1029/2008JD011681.
- Plummer, C. T., M. A. J. Curran, T. D. van Ommen, S. O. Rasmussen, A. D. Moy, T. R. Vance, H. B. Clausen, B. M. Vinther, and P. A. Mayewski (2012), An independently dated 2000-yr volcanic record from Law Dome, East Antarctica, including a new perspective on the dating of the 1450s CE eruption of Kuwae, Vanuatu, *Clim. Past*, *8*, 1929–1940, doi:10.5194/cp-8-1929-2012.
- Pósfai, M., J. R. Anderson, P. R. Buseck, and H. Sievering (1999), Soot and sulfate aerosol particles in the remote marine troposphere, *J. Geophys. Res.*, *104*(D17), 21,685–21,693, doi:10.1029/1999JD900208.
- Pósfai, M., R. Simonics, J. Li, P. V. Hobbs, and P. R. Buseck (2003), Individual aerosol particles from biomass burning in southern Africa: 1. Compositions and size distributions of carbonaceous particles, *J. Geophys. Res.*, *108*(D13), 8483, doi:10.1029/2002JD002291.
- Rothembacher, S., A. Messerer, and G. Kasper (2008), Fragmentation and bond strength of airborne diesel soot agglomerates, *Part. Fib. Toxicol.*, *5*(9), 1, doi:10.1186/1743-8977-5-9.
- Saunders, R. W., et al. (2010), An aerosol chamber investigation of the heterogeneous ice nucleating potential of refractory nanoparticles, *Atmos. Chem. Phys.*, *10*(3), 1227–1247, doi:10.5194/acp-10-1227-2010.
- Scarnato, B. V., S. China, K. Nielsen, and C. Mazzoleni (2015), Perturbations of the optical properties of mineral dust particles by mixing with black carbon: A numerical simulation study, *Atmos. Chem. Phys.*, *15*(12), 6913–6928, doi:10.5194/acp-15-6913-2015.
- Shen, Z., J. Liu, L. Horowitz, D. Henze, S. Fan, D. Mauzerall, J.-T. Lin, and S. Tao (2014), Analysis of transpacific transport of black carbon during HIPPO-3: Implications for black carbon aging, *Atmos. Chem. Phys.*, *14*(12), 6315–6327, doi:10.5194/acp-14-6315-2014.
- Slikboer, S., L. Grandy, S. L. Blair, S. A. Nizkorodov, R. W. Smith, and H. A. Al-Abadleh (2015), Formation of light absorbing soluble secondary organics and insoluble polymeric particles from the dark reaction of catechol and guaiacol with Fe(III), *Environ. Sci. Technol.*, *49*, 7793–7801, doi:10.1021/acs.est.5b01032.
- Slowik, J. G., et al. (2007), An inter-comparison of instruments measuring black carbon content of soot particles, *Aerosol Sci. Technol.*, *41*(3), 295–314, doi:10.1080/02786820701197078.
- Smith, A. J. A., and R. G. Grainger (2014), Simplifying the calculation of light scattering properties for black carbon fractal aggregates, *Atmos. Chem. Phys.*, *14*(15), 7825–7836, doi:10.5194/acp-14-7825-2014.
- Stohl, A., and H. Sodemann (2010), Characteristics of atmospheric transport into the Antarctic troposphere, *J. Geophys. Res.*, *115*, D02305, doi:10.1029/2009JD012536.
- van Ommen, T. D., and V. Morgan (1996), Peroxide concentrations in the Dome Summit South ice core, Law Dome, Antarctica, *J. Geophys. Res.*, *101*(D10), 15,147–15,152, doi:10.1029/96JD00838.
- Wang, X., C. L. Heald, D. A. Ridley, J. P. Schwarz, J. R. Spackman, A. E. Perring, H. Coe, D. Liu, and A. D. Clarke (2014), Exploiting simultaneous observational constraints on mass and absorption to estimate the global direct radiative forcing of black carbon and brown carbon, *Atmos. Chem. Phys.*, *14*(20), 10,989–11,010, doi:10.5194/acp-14-10989-2014.
- Warren, S. G., and A. D. Clarke (1990), Soot in the atmosphere and snow surface of Antarctica, *J. Geophys. Res.*, *95*(D2), 1811–1816, doi:10.1029/JD095iD02p01811.
- Weller, R., A. Minikin, A. Petzold, D. Wagenbach, and G. König-Langlo (2013), Characterization of long-term and seasonal variations of black carbon (BC) concentrations at Neumayer, Antarctica, *Atmos. Chem. Phys.*, *13*(3), 1579–1590, doi:10.5194/acp-13-1579-2013.
- Wolff, E. W., and H. Cachier (1998), Concentrations and seasonal cycle of black carbon in aerosol at a coastal Antarctic station, *J. Geophys. Res.*, *103*(D9), 11,033–11,041, doi:10.1029/97JD01363.
- Zhu, J., P. A. Crozier, and J. R. Anderson (2013), Characterization of light-absorbing carbon particles at three altitudes in East Asian outflow by transmission electron microscopy, *Atmos. Chem. Phys.*, *13*(13), 6359–6371, doi:10.5194/acp-13-6359-2013.